THE ASTROPHYSICAL JOURNAL, 460:644–650, 1996 April 1

VERY HIGH ENERGY GAMMA-RAY EMISSION FROM THE BLAZAR MARKARIAN 421

M. S. SCHUBNELL,[1] C. W. AKERLOF,[1] S. BILLER,[2] J. BUCKLEY,[3] D. A. CARTER-LEWIS,[4] M. F. CAWLEY,[5] M. CHANTELL,[3] V. CONNAUGHTON,[3,6] D. J. FEGAN,[6] S. FENNELL,[6] J. A. GAIDOS,[7] A. M. HILLAS,[2] A. D. KERRICK,[4,8] R. C. LAMB,[4] D. I. MEYER,[1] G. MOHANTY,[4] J. ROSE,[2] A. C. ROVERO,[3,9] G. SEMBROSKI,[7] T. C. WEEKES,[3] C. WILSON,[7] AND J. ZWEERINK[4]

Received 1995 March 22; accepted 1995 October 12

ABSTRACT

Very high energy gamma-ray emission from the BL Lacertae object Markarian 421 has been detected over three observing seasons on 59 nights between 1992 April and 1994 June with the Whipple 10 m imaging Cherenkov telescope. During its initial detection in 1992, its flux above 500 GeV was 1.6×10^{-11} photons cm^{-2} s^{-1}. Observations in 1993 confirmed this level of emission. For observations made between 1993 December and 1994 April, its intensity was a factor of 2.2 ± 0.5 lower. Observations on 1994 May 14 and 15 showed an increase over this quiescent level by a factor of ~ 10 (see paper by Kerrick et al.). This strong outburst suggests that four episodes of increased flux measurements on similar timescales in 1992 and 1994 may be attributed to somewhat weaker outbursts. The variability of the TeV gamma-ray emission from Mrk 421 stands in contrast to EGRET observations (see paper by Lin et al.), which show no evidence for variability.

Subject headings: BL Lacertae objects: individual (Markarian 421) — gamma rays: observations

1. INTRODUCTION

The central engines of active galactic nuclei (AGNs) are presumed to be massive black holes with accretion powers that radiate over a wide range of the electromagnetic spectrum. More than a score of these have now been reported as sources of multihundred MeV/GeV photons (Fichtel et al. 1994), all of which are identified with the subclass of AGNs that are radio loud and core dominated, and most of which are blazars. (See Dermer & Schlickeiser 1992 for a glossary of terms relevant to AGNs.)

The AGNs reported by EGRET vary in brightness by a decade and range in redshift from 0.031 to above 2. The nearest such object is Mrk 421, a BL Lac object extensively observed at radio (Owen et al. 1978; Zhang & Baath 1990), UV/optical (Maza, Martin, & Angel 1978; Mufson et al. 1990), and X-ray frequencies (Mufson et al. 1990; Mushotzky et al. 1979; George, Warwick, & Bromage 1988). Its parent galaxy has been identified as a giant elliptical (Ulrich et al. 1975; Mufson, Hutter, & Kondo 1989), and it was the first BL Lac object established as an X-ray source (Ricketts, Cooke, & Pounds 1976). Using VLBI techniques, the radio fine structure of the source has been mapped with a resolution of 1 mas to show a core-jet–like structure that exhibits possible superluminal motion (Zhang & Baath 1990). Variability with a timescale of hours has been observed in X-rays (Giommi et al. 1990) and at lower energies (Xie et al. 1988). Historically the source has exhibited low-amplitude variability on the scale of months to years in the radio emission (Aller & Aller 1995), but so far there is no evidence for variability in the gamma-ray emission in the high-energy regime (100 MeV to 10 GeV; Lin et al. 1994).

A comprehensive summary of recent theoretical work relevant to the blazars is given by von Montigny et al. (1995). Although the ultimate origin of the blazar power is the central engine, high-energy gamma-ray emission is likely to be beamed from a jet of highly relativistic particles. (If one assumes isotropy for the emission, enormous luminosities, in some cases more than 10^{49} ergs s^{-1} would be required.) Furthermore, any gamma rays at GeV to TeV energies that may be created in the inner regions of the source would be readily absorbed via the pair production process. Because of the likely jet geometry associated with the high-energy emission process, time variations observed at a single energy, if present, do not place strong constraints on the region of emission since there are many ways in which that variability may arise. However, correlated timescale variations at different energies (e.g., hard synchrotron and TeV) are generally useful and are the predicted consequence of models in which the gamma rays are produced by inverse Compton scattering.

It has been pointed out by Gould & Schréder (1967) and recently reformulated by several authors (Stecker, De Jager, & Salamon 1992; Salamon, Stecker, & De Jager 1994; Dwek & Slavin 1994; MacMinn & Primack 1995) that the interaction of gamma rays with intergalactic infrared and optical photons produced by galaxy formation may severely attenuate the TeV photon emission from cosmologically distant objects and that evidence for such absorption (or lack thereof) may be used to constrain both the energy density of starlight and the distance of the sources. The dynamic energy range covered by the Whipple Observatory instrument is particularly sensitive to such effects for the assumed distance to Mrk 421 (124 Mpc, $H_0 = 75$ km s^{-1} Mpc^{-1}) and an upper limit on the IR density field from our observation is derived in a separate paper (Biller et al. 1995).

2. INSTRUMENT AND OBSERVATIONS

The observations reported in this paper were carried out with the very high energy gamma-ray telescope (Cawley et

[1] University of Michigan, Ann Arbor, MI 48109.
[2] University of Leeds, Leeds LS2 9JT, UK.
[3] Whipple Observatory, Harvard-Smithsonian CfA, Amado, AZ 85645.
[4] Iowa State University, Ames, IA 50011.
[5] St. Patrick's College, Maynooth, Co. Kildare, Ireland.
[6] University College Dublin, Belfield, Dublin 4, Ireland.
[7] Purdue University, West Lafayette, IN 47907.
[8] Postal address: Department of Physics and Geology, Northern Kentucky University, Highland Heights, KY 41099.
[9] Postal address: Instituto de Astronomía y Física del Espacio, C. C. 67, Suc. 28, 1428 Buenos Aires, Argentina.

al. 1990) at the Whipple Observatory on Mount Hopkins in southern Arizona (31°41″ north, 110°53″ west, altitude = 2300 m). This 10 m diameter telescope images Cherenkov light from air showers on a hexagonal array of 109 fast photomultiplier tubes (PMTs) in the focal plane. The inner 91 2.86 cm diameter tubes of this high-resolution camera have a 0°.25 spacing. A surrounding outer ring of 18 5.08 cm diameter PMTs was replaced in 1993 August with a partial ring of 18 2.86 cm tubes.

The effective energy threshold E_{th}, above which there is 100% detection efficiency over the effective collection area, was determined to be 0.4 TeV by simulations for the 1988/1989 observing season. For later periods, an adjustment due to changes in mirror reflectivity and camera configuration was made by calibrating with the measured cosmic-ray rate R assuming a scaling behavior as $R \propto E_{th}^{-1.7}$ for the energy threshold E_{th}. An energy threshold of 400 GeV corresponds to an average count rate of 270 minute^{-1}. This scaling method can also be used to estimate gamma-ray event rates at different energy thresholds for a source with a power-law spectrum $E^{-\alpha}$ and known spectral index α. In the context of this paper, we assume for the photon emission from the Crab Nebula an integral energy spectrum of the form $E^{-1.4}$ as derived by Vacanti et al. (1992)

A shower image is recorded when at least m out of the inner 91 tubes exceed the hardware threshold of n photoelectrons. With the standard trigger condition ($m = 2$, $n = 50$) a typical trigger rate of 4–5 Hz with $E_{th} = 400$ GeV is obtained. All the observations were restricted to zenith angles less than 40° where, on the basis of our Crab Nebula observations, the rate variation with zenith angle is smaller than 10%. More detailed descriptions of the instrument and the Cherenkov light imaging technique can be found elsewhere (Cawley et al. 1990; Lewis 1990; Reynolds et al. 1993). The majority of the data were taken in a standard on/off tracking mode in which the source region and a background region are observed for equal times (usually 28 minutes). The location of the background region differs from that of the source region only in right ascension; thus both regions have the same zenith angle coverage. This procedure eliminates systematic effects introduced by the small variation in counting rate due to zenith angle changes.

For a well-established source such as Mrk 421, the effective observing time can be doubled by observing in an alternative mode in which the telescope always follows the source ("tracking mode"). Under these conditions, shower selection procedures, described below, are used to establish an appropriate value for the rate of background showers. Table 1 summarizes the varying detector parameters for the three observing periods between 1992 and 1994.

Data were processed following the standard Whipple analysis procedures (Reynolds et al. 1993) in which the Cherenkov light images are flat-fielded, cleaned, and characterized by simple image moment parameters (Hillas 1985). The shape of the approximately elliptical shower image and its location relative to the assumed source location in the image plane are specified by the parameters *width*, *length*, and *distance*. The fourth parameter, α, is defined to be the angle between the major axis of the shower image and a line from its centroid to the assumed source location in the image plane. For gamma-ray showers from a pointlike source, α should be near 0 degrees since the elliptical images point to the location of the source in the image plane.

Information on the shape and the orientation of the images is used to remove more than 99% of background cosmic-ray showers, while keeping a substantial fraction (≥ 0.5) of possible gamma-ray showers. For this analysis we applied the same discrimination values as we have for the selection of gamma-ray events from the Crab Nebula (0°.073 < width < 0°.150, 0°.16 < length < 0°.3, 0°.51 < distance < 1°.1, $\alpha < 15°$). This image selection procedure ("supercuts") was successfully applied to repeated observations of the Crab Nebula and has proved to be the most sensitive and reliable technique so far developed to discriminate gamma-ray events from the dominant hadronic background (Fegan et al. 1994).

Motivated by the detection of Mrk 421 by the EGRET instrument at GeV energies (Lin et al. 1992), observations with the 10 m reflector were made initially between 1992 March 24 and June 2 for a total of 445 minutes on-source and an equal amount of time off-source during eight clear nights. With the instrument operating at an effective energy threshold of 500 GeV, we obtained strong evidence for gamma-ray emission from the direction of the source (Punch et al. 1992).

In the fall of 1992, several instrumental improvements were made including the recoating of most of the mirror facets of the 10 m reflector. Preparations for operation in coincidence with the nearby new 11 m telescope (Schubnell et al. 1992) resulted in changes in the trigger conditions as well. These modifications had the effect of changing the optimum selection criteria used for selecting gamma-ray images and made it necessary to introduce an image size selection in software to adjust the energy thresholds similar to that used previously. This selection, which excludes images with a total number of less than 350 photo electrons, was chosen to reproduce the expected Crab gamma-ray rate at 500 GeV and not to optimize the signal. During the following winter (1992/1993), the AGN observation program was continued and from 1992 December to 1993 February 26, Mrk 421 was again observed on 10 clear nights for a total of 750 minutes.

For the most recent observations, between 1993 Decem-

TABLE 1

INSTRUMENT PARAMETER

Season	Mode	E_{th} (GeV)	Collection Area (cm^2)	Trigger
1991–1992.....	On/off	500	3.5×10^8	$m = 2$, $n = 50$
1992–1993.....	On/off	400	2.2×10^8	$m = 3$, $n = 36$
1993–1994.....	On/off, tracking	350	3.5×10^8	$m = 2$, $n = 30$–40
1993–1994 (LC)[a].....	On/off, tracking	250	3.5×10^8	$m = 2$, $n = 30$–40

[a] Observations with light cones installed.

ber 16 and 1994 June 12, the mirror recoating was completed and the trigger condition reverted to that of previous years. The instrument was operating at an energy threshold of 350 GeV, somewhat lower than in 1988/1989 as a result of the higher mirror reflectivity. Prior to the observations in 1994 May, we installed light focusing cones in front of the PMT plane (Kerrick et al. 1995b). This increased the number of Cherenkov photons collected by the photomultipliers and decreased the trigger energy threshold. Observations with the light cones in place produced stable trigger rates and first measurements on the Crab Nebula showed a significant increase in the observed gamma-ray rate. Encouraged by these results, we have continued to use the light cones throughout the entire observing season as well as in 1994/1995 with reproducible results on the Crab Nebula, consistent with a 250 GeV energy threshold.

For the purpose of calculating the photon flux values and to investigate possible time variations, we reference all fluxes to the observed intensity of the Crab Nebula. This procedure corrects for possible systematic variations that are due to the different trigger conditions over the entire observing period, assuming the uniformity of the Crab emission. An analysis of the 4 yr data base of Crab Nebula observations shows that the flux is constant to better than 10% (Weekes et al. 1993). This limit of variability is included as a systematic error of 10% to the calculated Mrk 421 fluxes.

3. RESULTS

Because of the changes in the instrument as discussed in the previous section we will treat each of the observing seasons separately. The sensitivity of the Whipple telescope is such that a significant flux of 0.3 of the Crab flux can be observed from a single night's observations. Therefore the data set has been divided into daily intervals, with each interval spanning a minimum of $\frac{1}{2}$ hour observation. A summary of the observations for the three seasons reported here can be found in Table 2.

3.1. *The 1992 Season*

The first observation of very high energy gamma-ray emission from Mrk 421 was based on data taken during the 1992 March–June period (Punch et al. 1992). We reanalyzed this data set using the standard image analysis procedure but slightly modified the algorithm to calculate the relative photomultiplier gains and excluded phototubes for which the pedestal distributions were outside the statistical expectation. With the definition of the gamma-ray signal as $(N_{on} - N_{off})$, where N_{on} represents the number of selected images according to the discrimination procedure discussed in the previous section in the on-source scan and N_{off} represents the number of selected images in the off-source observation, we obtain an average gamma-ray rate of 0.34 ± 0.05 minute^{-1} over the total 445 minutes of observation. With the statistical significance σ defined as $(N_{on} + N_{off})^{1/2}$, we find that the observed excess has a significance of 6.7 σ.

Figure 1*a* shows how the difference $N_{on} - N_{off}$ is distributed as a function of the orientation parameter α after applying all other selection criteria. The excess at small α values is expected for gamma-ray events from the source direction, while hadron-initiated Cherenkov events are random in orientation and contribute an isotropic background. Assuming an effective area of 3.5×10^8 cm^2, the measured rate is equivalent to an integral gamma-ray flux of $1.59 \pm 0.20 \times 10^{-11}$ cm^{-2} s^{-1} above 500 GeV (see Table 3).

Two stars (SAO 62387 and SAO 62393) with a combined brightness equivalent to magnitude 5 are located near the Mrk 421 position. This led us to investigate the possibility of a false signal due to the brightness variation in "on" and "off" fields. The angular separation from Mrk 421 is on the order of the telescope's optical resolution, and thus both star images are always contained in the center tube. The most obvious test is to exclude the photomultiplier tube containing these stars (the center tube) from the analysis. No significant difference in the result was found. When we excluded the center tube from the trigger and the analysis during observations made in the following years, we also could find no evidence for a systematic effect. Additional control observations on two stars of similar magnitude show null results when subjected to the supercuts analysis.

Figure 2*a* shows the emission on a nightly basis for the 1992 observing period. The errors shown are statistical only and do not incorporate small systematic effects due to the variation in zenith angle of the observations. The maximum deviation (2.9 σ) from a steady flux is found on MJD 48764 (1992 May 22 UT). A χ^2 test of the 1992 data gives a 2% probability that the observed flux is consistent with constant emission (see Table 4).

If we exclude the observation from MJD 48764 from the sample and repeat the χ^2 test on the Mrk 421 data, the probability for constant observed emission then increases from 2% to 40%. We emphasize that the observed increase in photon emission on MJD 48764 has a marginal significance but, in context with the later observed day-scale flux variations, has to be considered as a likely flare. The apparent photon flux for this particular 38 minute observation is $5.0 \pm 1.2 \times 10^{-11}$ cm^{-2} s^{-1} above 500 GeV.

To exclude possible systematic effects in the instrument as the source for the variability in the emission, we have analyzed contemporaneous data from the Crab Nebula (Fig. 3*a*). From this we extract a gamma-ray rate of

TABLE 2

OBSERVATION SUMMARY

Observation Period	E_{th} (GeV)	Mode	Duration (minutes)	Nights	Gamma-Ray Rate (minute^{-1})
1992 Mar 24– Jun 2 1992.....	500	On/off	445	8	0.33 ± 0.05
1992 Dec 23–1993 Feb 26.....	400	On/off	750	10	0.29 ± 0.08
1993 Dec 15–1994 May 9	350	On/off	1145	16	0.31 ± 0.06
1994 Jan 10–May 3	350	Tracking	939	9	0.17 ± 0.06
1994 Jan 17–June 12.....	250	On/off	665	15	0.88 ± 0.14
1994 Mar 5–May 30.....	250	Tracking	516	5	1.47 ± 0.20

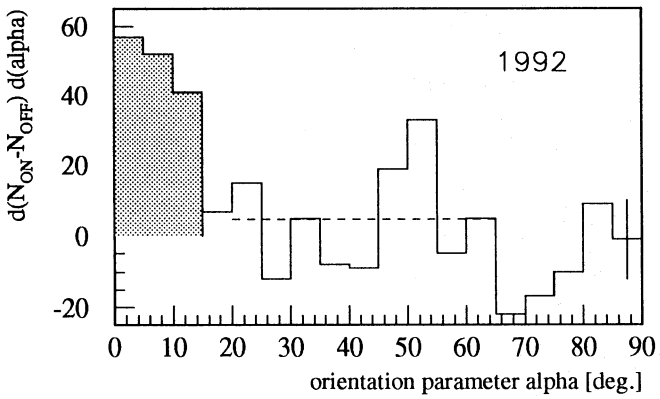

FIG. 1*a*

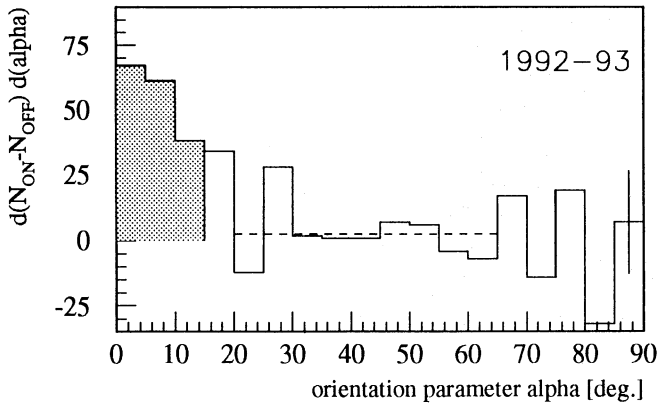

FIG. 1*b*

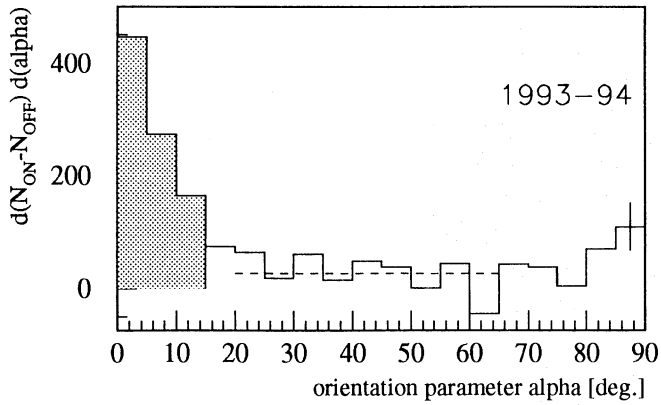

FIG. 1*c*

FIG. 1.—On-source minus off-source orientation angle (α) distributions for the three viewing periods: (*a*) 1992, (*b*) 1992/1993, and (*c*) 1993/1994. The net excess in gamma-ray like events accepted by the selection procedure is indicated by the shaded area. The dashed line shows the average net gamma-ray rate for images with large α angles. This rate is expected to be zero. A 1 σ statistical error bar is always shown for the bin 85°–90°.

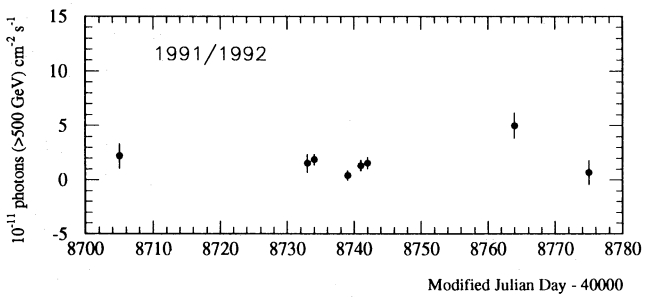

FIG. 2*a*

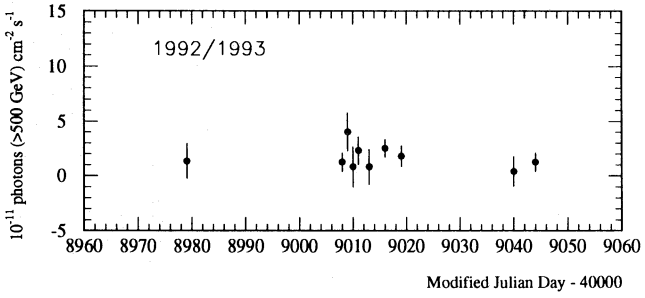

FIG. 2*b*

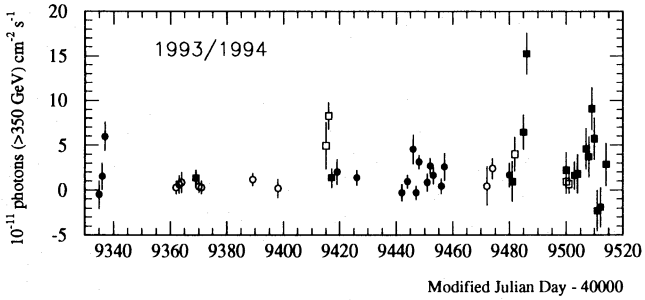

FIG. 2*c*

FIG. 2.—The observed fluxes from Mrk 421 for the three viewing seasons: (*a*) 1992, (*b*) 1993, and (*c*) 1994. Each data point corresponds to one night of observation. Different symbols indicate different instrument parameter and operation mode: *solid circle*, on/off mode, no light cones; *open circle*, tracking mode, no light cones; *solid square*, on/off mode, light cones; *open square*, tracking mode, light cones.

0.80 ± 0.08 minute^{-1} corresponding to an integral photon flux of $3.81 \pm 0.03 \times 10^{-11}$ cm^{-2} s^{-1} above 500 GeV. A χ^2 test for constant flux from the Crab Nebula gives a 48% probability.

3.2. *The 1992/1993 Season*

For the 1992/1993 season, changes in the trigger conditions (Table 1) resulted in a loss in effective collection area in spite of the fact that a large fraction of the mirrors had been recoated. In order to have a consistent data base for

TABLE 3

AVERAGE SEASON FLUXES

Observing Season	E_{th} (GeV)	Flux (cm^{-2} s^{-1})
1991/1992	500	$1.59 \pm 0.20 \times 10^{-11}$
1992/1993	500	$1.47 \pm 0.30 \times 10^{-11}$
1993/1994 preburst	350	$1.18 \pm 0.20 \times 10^{-11}$
1993/1994 burst	250	$21.90 \pm 3.80 \times 10^{-11}$
1993/1994 postburst	250	$2.48 \pm 0.60 \times 10^{-11}$

TABLE 4

PROBABILITY FOR CONSTANT EMISSION

Observing Season	Markarian 421 Probability	χ^2	ndf	Crab Nebula Probability
1991/1992	1.9×10^{-2}	16.8	7	0.48
1992/1993	0.84	5.0	9	0.66
1993/1994 preburst	1.3×10^{-9}	97.4	28	0.78
1993/1994 postburst	0.11	15.6	10	No data

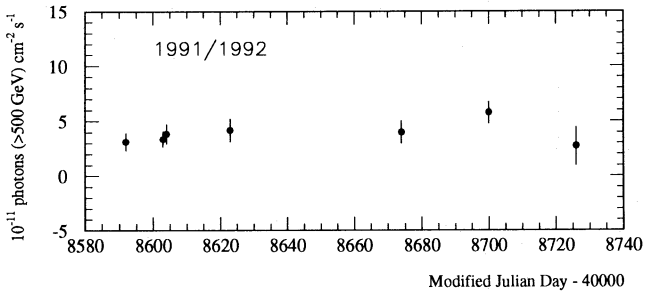

FIG. 3*a*

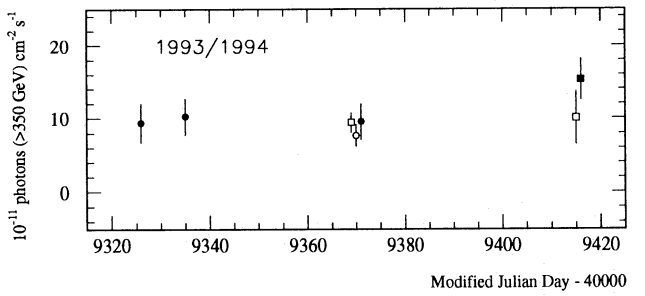

FIG. 3*b*

FIG. 3.—The observed fluxes from the Crab Nebula for the viewing seasons (*a*)1992 and (*b*) 1994. Symbols as in Fig. 2.

Mrk 421 for 1993, we have used only that data for which contemporaneous Crab observations under identical instrumental conditions are available as reference. Two instrumental effects had to be considered for the data analysis: (1) a new PMT camera with slightly different tube spacing was installed and (2) a persistent problem with one tube led to a software filtering procedure to remove triggers associated with that tube.

Following the above selection, a total of 750 minutes of on-source observations of Mrk 421, distributed over 10 nights, was obtained. Applying the standard analysis, we obtain an average gamma-ray rate of 0.29 ± 0.08 minute^{-1} with a significance level of 3.7 σ above 400 GeV.

From the observations of the Crab Nebula, we determined that a large portion of the trigger-induced background can be suppressed if we restrict the analysis to images with a total of at least 350 photoelectrons. This selection increases the effective energy threshold to 500 GeV. The corresponding on-off α distribution (with the 350 photoelectron cut applied) is shown in Figure 1*b*.

Although we have almost doubled the observing time compared to the 1992 season, the significance in the extracted signal is considerably lower due to the increased contamination of the selected gamma-ray sample with hadronic showers (signal/background = 0.29 compared to signal/background = 0.85 for the 1992 observations). The observed average gamma-ray rate is equivalent to an integral flux of $1.67 \pm 0.4 \times 10^{-11}$ cm^{-2} s^{-1} above 500 GeV, in good agreement with the result from the previous year if we scale the 400 GeV 1992 result to 500 GeV, assuming an integral spectrum like E^{-1}. (The assumption of an integral spectrum E^{-1} for Mrk 421 in this context is justified by the extrapolation of the [integral] 1992 flux to the lower energy EGRET data points [Lin et al. 1994].)

The nightly flux values were calculated to test for variability of the emission (Fig. 2*b*). The maximum deviation (1.3 σ) from a steady flux is found on MJD 49009 (1993 January 22 UT). A χ^2 test gives a 84% probability that the flux is constant (Table 4).

3.3. *The 1994 Season*

In an effort to monitor more closely the photon emission from Mrk 421, extensive observations were taken during the period 1993 December 15–1994 June 12 (MJD 49336–49515). The instrument operated with two slightly different energy thresholds, depending on whether or not light-focusing cones were in place. All the scans prior to May 10 were taken without the light cones with the exception of observations on January 17 (MJD 49369), March 5 (MJD 49415), and March 6 (MJD 49416). For the runs without the light cones, the energy threshold is already significantly lower ($E_{th} = 350$ GeV) than for the previous year, an improvement due to the higher reflectivity of the newly coated mirrors. The energy threshold for observations with the light cones is $E_{th} = 250$ GeV.

During the night of May 15 (MJD 49487) an increase by a factor of 9 in the Mrk 421 TeV emission was observed (Kerrick et al. 1995a). Because of the occurrence of this outburst we separate the observations into preburst, burst, and postburst periods.

3.3.1. *Preburst*

For observations in the standard on/off mode between 1993 December and 1994 April we measured an average gamma-ray rate of 0.31 ± 0.06 minute^{-1} during 1145 minutes, on 16 nights with a significance of 5.5 σ (Table 2). The energy threshold during this period is calculated from contemporaneous Crab observations ($R_{Crab} = 1.89$ minute^{-1}) to be 350 GeV. In addition, we obtained observations without the light cones in tracking mode on nine nights totaling 939 minutes, resulting in an average gamma-ray rate of 0.17 ± 0.06. During four nights in which light cones were in place, we collected an almost equal amount of tracking mode and on/off mode data (Table 2). The average observed gamma-ray rate is 1.59 ± 0.18. From Table 2 and Figure 2*c* it can be seen that this high average rate is due to an increase in the observed emission on March 5 and 6. For the night of March 6, we have observations of the Crab Nebula that we analyzed to exclude the possibility of systematic effects that could be attributed to either the newly mounted light cones or the nonstandard observing technique (tracking) for those two nights. On 1994 March 6, we observed the Crab Nebula for 29 minutes under identical instrumental conditions as for the Mrk 421 observations. The detected gamma-ray rate is 2.9 ± 1.1 minute^{-1}, in agreement with the average of 3.35 ± 0.39 minute^{-1} for all the Crab Nebula scans at the 250 GeV energy threshold. In the absence of any other systematic effect (for example, unstable weather conditions) the observed excess is statistically significant. A χ^2 test applied to all preburst data gives a probability of 1.3×10^{-9}. The largest contribution comes from March 6 (see Fig. 2*c*). The average gamma-ray rate for the preburst period (excluding March 6) for the combined data between 1993 December 15 (MJD 49336) and 1994 May 9 (MJD 49481) is 0.23 ± 0.04 minute^{-1} above 350 GeV. If we scale from the average of the 1992 and 1993 observing season (0.32 minute^{-1}), we expect a rate of 0.50 minute^{-1} above 350 GeV. Even if we allow an additional systematic error of 10%, the constant emission from Mrk 421 between 1993 December and 1994 May is, by a factor of 2.2 ± 0.5, significantly below that of the two previous observing seasons.

3.3.2. *Burst*

While on May 9 (MJD 49419), Mrk 421 was still observed at the low flux level of the previous months, a significant increase of the photon flux was observed on May 15 (MJD 49487; see Fig. 2*c*), reaching a maximum of 2.1×10^{-10} cm^{-2} s^{-1} during a 28 minute scan (Kerrick et al. 1995a). During this observation we measured a gamma-ray event rate at the level of 4.5 ± 0.8 minute^{-1}, a rate comparable to the Crab at this energy level. The appearance of the Moon during the following nights made observations of Mrk 421 impossible again until May 30 (MJD 49502). The TeV outburst of Mrk 421 occurred during a multiwavelength campaign, and simultaneous or contemporaneous observations are available. The strongest observed TeV flux precedes the observation of an increase in the hard X-ray emission by the *ASCA* satellite by 24 hours (Takahashi et al. 1994). Simultaneous observations by the EGRET instrument did not indicate an increase in the GeV emission. A detailed analysis of the multiwavelength data is discussed in a separate paper (Macomb et al. 1995).

3.3.3. *Postburst*

Following the outburst in May, we monitored Mrk 421 during the month of June when permitted by weather and Moon. All observations were made in the standard on/off mode with light cones in place. The average observed gamma-ray rate is 0.43 ± 0.13 minute^{-1} over the course of 10 nights (see Fig. 2*c*) with a probability of 11% for constant emission (see Table 4).

The average integral photon fluxes measured at 250 and at 500 GeV are consistent with the extrapolation of the spectrum measured between 100 MeV and several GeV (see Fig. 4). As of the time this paper was written, no detection of gamma rays from Mrk 421 has been claimed by experiments sensitive to gamma-ray energies above 10 TeV. Reported upper limits on the photon emission from those experiments (Alexandreas et al. 1993; Amenomori et al. 1994; Catanese et al. 1994; Karle 1994; Kühn 1994) have been incorporated in Figure 4.

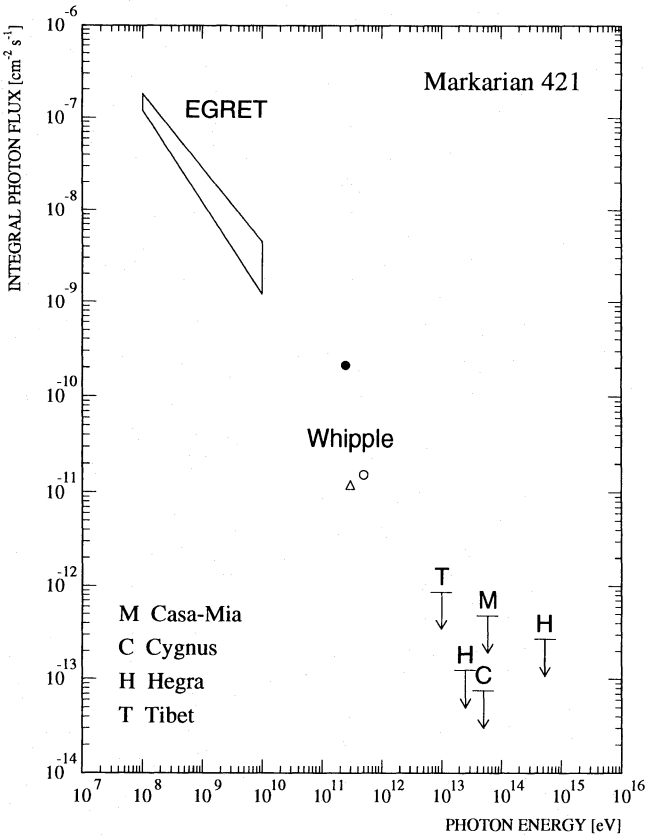

FIG. 4.—Integral photon spectrum for Mrk 421. The error box for EGRET was converted from the differential fit to the observed data (Lin et al. 1993). Upper limits are from air shower experiments: HEGRA (Karle 1994; Kühn 1994); Cygnus (Alexandreas et al. 1993); Tibet (Amenomori et al. 1994); CASA-MIA (Catanese et al. 1994). The Whipple data points are the average integrated flux for 1992 and 1992/1993 (*open circle*), the preburst average flux in 1994 (*open triangle*), and the flux observed during the burst in 1994 May (*solid circle*).

4. DISCUSSION

The average gamma-ray flux observed during 1992 and 1993 corresponds to a photon luminosity of $\sim 10^{43}$ ergs s^{-1} above 500 GeV, assuming isotropic emission at a distance of 124 Mpc. However, the fact that all identified extragalactic sources detected by EGRET can be associated with the blazar class of AGNs suggests that the GeV emission is highly beamed, originating in the relativistic plasma outflow that forms the radio jets. Beamed emission of the gamma rays furthermore overcomes the strong photon-photon absorption implied by the large gamma-ray luminosities for the case of isotropic emission. If we adopt the picture of beamed emission for the TeV component, the true VHE gamma-ray luminosity decreases by a factor of $\sim 10^{-3}$ for beam opening angles of the order of a few degrees.

Much attention has been devoted lately to the discussion of possible absorption of the TeV photons in the intergalactic radiation field (Stecker et al. 1992; Salamon et al. 1994), i.e., gamma rays with energies of 0.5–5 TeV interacting with soft 0.05–0.5 eV photons to produce e^+e^- pairs. For a relatively nearby source like Mrk 421 ($z = 0.031$) this is a rather small effect. (The possible presence of an absorption effect in our original 1992 data [Mohanty et al. 1993] has been used by De Jager et al. [1994] to determine a value for the infrared energy density. A more conservative approach has been adopted by Biller et al. 1995 to establish an upper limit to the energy density.)

The question arises of whether or not this process could be occurring in the vicinity of the AGN, that is to say, can gamma rays with TeV energies escape the photon field close to the central engine of the AGN? For some models this requirement is a severe obstacle, as explained for instance by Coppi, Kartje, & Königl (1993). While their theory nicely models the nonthermal emission component by upscattering radiation (ambient or synchrotron–self-Compton produced) by a relativistic electron/proton beam, they need to place the TeV emission regime further from the core than the GeV emission in order to avoid absorption in the region of high-energy density at small distances. In simultaneous observations during the 1994 May TeV outburst (Macomb et al. 1995), the EGRET instrument did not observe an increase in the photon emission from Mrk 421 above the previously detected level (Lin et al. 1994).

Many of the various models that have been proposed to explain the origin of the gamma-ray emission favor production of the gamma-rays by the inverse-Compton process. Beamed relativistic electrons in the jet upscatter low-energy photons from synchrotron radiation (Ghisellini & Maraschi 1989; Marscher & Bloom 1992) or other ambient sources (Blandford 1993; Dermer, Schlickeiser, &

Mastichiadis 1992; Sikora, Begelman, & Rees 1994) to gamma-ray energies. These models imply a strong correlation between the production of radiation across the nonthermal waveband. Any change in the electron flow or electron distribution translates into a variation in the emission at other wavelengths. Differences in the relation of variability at given frequencies reflect distinct production regions.

The inhomogeneous synchrotron–self-Compton model by Maraschi, Ghisellini, & Celotti (1992), for instance, places the production of gamma rays at the inner part of the jet while hard X-rays (as well as radio and IR emission) are produced in the outer jet part, and thus fluctuations in the gamma-ray band are predicted to lead X-ray variability by typically a day.

In a similar model by Sikora, Begelman, & Rees (1994), the entire gamma-ray spectrum is produced within the same jet region through Comptonization of ambient radiation (from dust near the jet) by relativistic electrons. The authors point out that the problem of TeV opaqueness can be overcome if the seed photons come from thermal IR emission by dust rather than UV photons. They are supported by the fact that while thermal UV excess is common for OVV quasars, it is observed in only very few BL Lac objects. This hints that the nonobservation of EGRET detected sources other than Mrk 421 (Kerrick et al. 1995b) above a few hundred GeV may be a combination of an intrinsic source feature (BL Lac objects vs. OVVs, for example) and the increasing IR absorption toward higher redshifts. Clearly, this needs more observational evidence, some of which can be provided by future measurements of AGN emission spectra in the 10–100 GeV regime where both processes will potentially cut off the power-law spectrum observed at high energies.

In contrast to the leptonic models is the approach by Mannheim (Mannheim 1993; Mannheim & Biermann 1992) in which a shock-accelerated ultrarelativistic proton population in the jet photoproduces π^0, and the observed gamma rays are then produced by synchrotron cascade reprocessing. In this model, the gamma-ray emission observed at GeV energies extends naturally into the TeV regime. No predictions about the correlation of variability in the TeV gamma-ray emission to the GeV and X-ray emission are made, but it was pointed out by von Montigny et al. (1995) that a disturbance in the proton population can translate to large gamma-ray flares downstream from the cascade origin.

Although the Whipple collaboration has recently reported a somewhat weaker TeV AGN source, Mrk 501 (Quinn et al. 1995), Mrk 421 is, so far, the best probe to test models at the highest accessible energies.

The detection of a TeV component in the Mrk 421 emission as well as the observation of day scale variability already constrains models of gamma-ray production in relativistic jets. Additional, extended simultaneous observations of Mrk 421 over the optical, UV, GeV, and TeV energy regime are crucial to establish the correlations of nonthermal photon emission with the ultimate goal of understanding the gamma-ray production and emission process in blazars.

We thank Kevin Harris and Teresa Lappin for their considerable help in obtaining the observations. The Whipple Collaboration acknowledges support from the US Department of Energy, NASA, the Smithsonian Scholarly Studies Research Fund, and EOLAS, the scientific funding agency of Ireland. S. B. acknowledges the financial support of the National Science Foundation.

REFERENCES

Alexandreas, D. E., et al. 1993, ApJ, 418, 832
Aller, H. D., & Aller, M. F 1995, private communication
Amenomori, M., et al. 1994, ApJ, 429, 634
Biller, S. D., et al. 1995, ApJ, 445, 227
Blandford, R. D. 1993 in AIP Conf. Proc., No. 280, *Compton Gamma Ray Observatory*, ed. M. Friedlander, N. Gehrels, & D. J. Macomb (New York: AIP), 533
Catanese, M., et al. 1994, in Proc. 8th Meeting, Div. of Particles and Fields of the American Phys. Soc., ed. S. Seidel (Singapore: World Scientific), 129
Cawley, M. F., et al. 1990, Exp. Astron., 1, 173
Coppi, P. S., Kartje, J. F., & Königl, A. 1993, in AIP Conf. Proc., No. 280, *Compton Gamma Ray Observatory*, ed. M. Friedlander, N. Gehrels, & D. J. Macomb (New York: AIP), 559
Dermer, C. D., & Schlickeiser, R. 1992, Science, 257, 1642
Dermer, C. D., Schlickeiser, R., & Mastichiadis, A. 1992, A&A, 256, L27
Dwek, E., & Slavin, J. 1994, ApJ, 436, 696
Fegan, D. 1994 in UAP Conf. Proc. 13, Towards a Major Atmospheric Cerenkov Detector III, ed. T. Kifune (Tokyo: Universal Acad. Press), 149
Fichtel, C. E., et al. 1994, ApJS, 94, 551
George, U. M., Warwick, R. S., & Bromage, G. E. 1988, MNRAS, 232, 793
Ghisellini, G., & Maraschi, L. 1989, ApJ, 340, 181
Giommi, P., et al. 1990, ApJ, 356, 432
Gould, R. J., & Schreder, G. P. 1967, Phys. Rev., 155, 1408
Hillas, A. M. 1985, in Proc. 19th Internat. Cosmic Ray Conf. (La Jolla), 3, 445
Karle, A. 1994, Ph.D. thesis, Munich MPI-PhE/94-17
Kerrick, A. D., et al. 1995a, ApJ, 438, L59
———. 1995b, ApJ, 452, 588
Kühn, M. 1994, Ph.D. thesis, Univ. of Kiel
Lewis, D. A. 1990, Exp. Astron., 1, 213
Lin, Y. C., et al. 1992, ApJ, 401, L61
———. 1994, in AIP Conf. Proc., No. 304, 2d Compton Symp., ed. C. E. Fichtel, N. Gehrels, & J. F. Norris (New York: AIP), 582
MacMinn, D., & Primack, J. 1995, preprint
Macomb, D. J., et al. 1995, ApJ, 449, L99
Mannheim, K. 1993, A&A, 269, 67
Mannheim, K., & Biermann, P. L 1992, A&A, 253, L21
Maraschi, L., Ghisellini, G., & Celotti, A. 1992, ApJ, 397, L5
Marscher, A. P., & Bloom, S. D. 1992 in AIP Conf. Proc., No. 304, 2d Compton Symp., ed. C. E. Fichtel, N. Gehrels, & J. F. Norris (New York: AIP), 572
Maza, J., Martin, P. G., & Angel, J. R. P. 1978, ApJ, 224, 368
Mufson, S. L., Hutter, D. J., & Kondo, Y. 1989, in BL Lac Objects, ed. L. Maraschi, T. Maccacaro, & M.-H. Ulrich (Berlin: Springer), 341
Mufson, S. L., et al. 1990, ApJ, 354, 116
Mushotzky, R. F., Boldt, E. A., Holt, S. S., & Serlemitsos, P. J. 1979, ApJ, 232, L17
Owen, F. N., Porcas, R. W., Mufson, S. L., & Moffet, T. J. 1978, ApJ, 83, 685
Punch, M., et al. 1992, Nature, 358, 477
Quinn, J., et al. 1995, IAU Circ., No. 6178
Reynolds, P. T., et al. 1993, ApJ, 404, 206
Ricketts, M. J., Cooke, B. A., & Pounds, K. A. 1976, Nature, 259, 546
Salamon, M. H., Stecker, F. W., & De Jager, O. C. 1994, ApJ, 390, L49
Schubnell, M. S., et al. 1992, in AIP Conf. Proc. No. 280, *Compton Gamma Ray Observatory*, ed. M. Friedlander, N. Gehrels, & D. J. Macomb (New York: AIP), 1171
Sikora, M., Begelman, M. C., & Rees, M. J. 1994 ApJ, 421, 153
Stecker, F. W., De Jager, O. C., & Salamon, M. H. 1992, ApJ, 390, L49
Takahashi, T., et al. 1994, IAU Circ., No. 5993
Ulrich, M.-H., Kinman, T. D., Lynds, C. R., Rieke, G. H., & Ekers, R. D. 1975, ApJ, 198, 261
Vacanti, G., et al. 1991, ApJ, 377, 467
von Montigny, C., et al. 1995, ApJ, 440, 525
Weekes, T. C., et al. 1993, in AIP Conf. Proc., No. 304, 2d Compton Symp., ed. C. E. Fichtel, N. Gehrels, & J. F. Norris (New York: AIP), 270
Xie, G. Z., et al. 1988, A&AS, 72, 163
Zhang, F. J., & Baath, L. B. 1990, A&A, 236, 47